Endocrine Journal

Advance Publication
doi:10.1507/endocrj.EJ19-0271

ORIGINAL

Circular RNA HIPK3 contributes to hyperglycemia and insulin homeostasis by sponging miR-192-5p and upregulating transcription factor forkhead box O1

Huiyao Cai, Zhengrong Jiang, Xinna Yang, Jiayu Lin, Qingyan Cai and Xisheng Li

Department of Endocrinology, The Second Affiliated Hospital of Fujian Medical University, Quanzhou City, Fujian Province, 362000, China

Abstract. It has been shown that circular RNAs, a class of non-coding RNA molecules, play an important role in the regulation of glucose and lipid homeostasis. In the present study, we sought to investigate the function of circular RNA HIPK3 (circHIPK3) in diabetes-associated metabolic disorders, including hyperglycemia and insulin resistance. Results show that oleate stimulated circHIPK3 increase, and that circHIPK3 enhanced the stimulatory effect of oleate on adipose deposition, triglyceride (TG) content, and cellular glucose content in HepG2 cells. MiR-192-5p was the potential target of circHIPK3, since circHIPK3 significantly decreased miR-192-5p mRNA level, whereas anti-circHIPK3 significantly increased miR-192-5p mRNA level. Further study shows that transcription factor forkhead box O1 (FOXO1) was a downstream regulator of miR-192-5p, since miR-192-5p significantly decreased FOXO1 expression, whereas circHIPK3 significantly increased FOXO1 expression. Notably, the inhibitory effect of miR-192-5p was significantly reversed by circHIPK3. *In vivo* study shows that anti-miR-192-5p significantly increased blood glucose content, which was significantly inhibited by FOXO1 shRNA. MiR-192-5p significantly decreased adipose deposition and TG content in HepG2 cells, which was significantly reversed by the co-treatment with circHIPK3. Forskolin/dexamethasone (FSK/DEX) significantly increased cellular glucose, mRNA level of phosphoenolpyruvate carboxykinase (PEPCK) and glucose 6-phosphatase (G6Pase), and this stimulatory effect of FSK/DEX was significantly inhibited by miR-192-5p. In the presence of circHIPK3, however, the inhibitory effect of miR-192-5p was totally lost. In summary, the present study demonstrated that circHIPK3 contributes to hyperglycemia and insulin resistance by sponging miR-192-5p and up-regulating FOXO1.

Key words: MiR-192-5p, Circular HIPK3, Forkhead box O1, Hyperglycemia, Insulin resistance

CIRCULAR RNAS (CIRCRNAS), without cap and polyA tails, forms covalently closed continuous loops by non-sequential back-splicing of pre-mRNA transcripts [1]. CircRNAs are resistant to degradation since they are resistant to exonuclease, the property of which makes circRNAs superior than linear RNAs in terms of biological markers [2]. Till now, various properties of circRNAs have been identified in recent years, and "miRNA sponges" was the most studied [3, 4]. It has been reported that circHIPK3 directly binds to miR-124 and inhibits miR-124 activity [5]. However, the role of circHIPK3 remains largely unknown.

It has been well documented that forkhead box O1 (FOXO1) is a key insulin signaling downstream negative regulator and plays a significant role in regulating glucose homeostasis [6]. At physiological conditions, the insulin receptor (IR)/phosphatidylinositol-3-kinase (PI3K)/Akt signaling pathway is activated by insulin, which then phosphorylates FOXO1, resulting in its nuclear exclusion and suppression of its transcriptional activity. During fasting, however, FOXO1 promotes gluconeogenesis in the liver by inducing the expression of phosphoenolpyruvate carboxykinase (PEPCK) and glucose 6-phosphatase (G6Pase), and by inducing a transition from carbohydrate oxidation to lipid oxidation in the liver [7]. Therefore, mice overexpressing FOXO1 in the liver exhibited hyperglycemia, hyperinsulinemia, hypertriglyceridemia and hepatosteatosis [8, 9]. Furthermore, FOXO1 targets genes responsible for lipogenesis, including sterol regulatory element binding protein 1c (SREBP-1c) and fatty acid synthase (FAS) [8, 10, 11]. After proteolytic cleavage, the mature N-terminal SREBP-1c translocates into the nucleus, where it binds

Submitted Jun. 28, 2019; Accepted Nov. 20, 2019 as EJ19-0271
Released online in J-STAGE as advance publication Dec. 24, 2019
Correspondence to: Huiyao Cai, Department of Endocrinology, The Second Affiliated Hospital of Fujian Medical University, 950 Donghai Street, Fengze district, Quanzhou City, Fujian Province, 362000, China.
E-mail: caihyshfjmu@126.com

©The Japan Endocrine Society

to serum response elements (SREs) of the FAS promoter. Through this mechanism, insulin signals may up-regulate FAS in the liver. Indeed, FAS expression, as well as, that of SREBP-1c is reportedly increased in subjects with nonalcoholic fatty liver disease (NAFLD) [12].

It has been documented that FOXO1 is regulated by miRNA. For example, it has been reported that miR-96-5p inhibited autophagy *via* downregulation of the expression of FOXO1 and acetylated-FOXO1 in human breast cancer cell [13]. However, the relationship between circHIPK3 and FOXO1/diabetes remains largely unknown. We then performed bioinformatics analysis and found that circHIPK3 could bind miR-192-5p, and miR-192-5p could bind FOXO1 mRNA. Of note, it has been reported that circulating miR-192 and miR-194 are associated with the presence and incidence of diabetes mellitus [14]. In the present study, we hypothesized that circHIPK3-miR-192-5p-FOXO1 signaling pathway may contribute to hyperglycemia and insulin resistance.

Materials and Methods

Cell culture

Human hepatocellular carcinoma HepG2 cells and Huh7 cells were cultured in Dulbecco's modified Eagle's medium (DMEM) (Gibco, Waltham, MA, USA) supplemented with 10% fetal bovine serum (FBS, Gibco) and 233.6 mg/mL glutamine. AML12 cells, a mouse hepatocyte cell line, were grown in DMEM/F-12 medium (Gibco) supplemented with 10% FBS, 1 × insulin-transferrin-seleniums (Gibco), 40 ng/mL dexamethasone, and 233.6 mg/mL glutamine. Cells were maintained at 37°C in a humidified atmosphere containing 5% CO_2 [15]. Some cells were treated with oleate (200 μM) to mimic the effect of unsaturated fatty acid, and some cells were treated with forskolin (FSK, 10 μM, Sigma-Aldrich, St. Louis, MO, USA), and dexamethasone (DEX, 100 nM, Sigma-Aldrich) to mimic the action of glucagon and glucocorticoids [8].

Bioinformatics assay

The potential binding miRNAs with circHIPK3 were evaluated with Circular RNA Interactome (https://circinteractome.nia.nih.gov/) as described on the website. The potential binding sites of miR-192-5p with mRNAs were evaluated online (http://genie.weizmann.ac.il/pubs/mir07/mir07_prediction.html), and the binding bases with 7 bp or more were viewed as positive.

Oil Red O staining

The Oil Red O staining was used for determining lipid droplets [16]. Cells were washed with PBS and fixed with 4% paraformaldehyde for 30 min, then cells were stained with 5% Oil Red O for 30 min and hematoxylin for 2 min. The sections were observed with a magnification of 100× and 200× (Leica, Wetzlar, Hesse, Germany).

Construction of adenovirus

The full length of circHIPK3 was used as circHIPK3 mimics (Supplementary data). The circHIPK3 inhibitor sequence was 5'-ACTACAGGTATGGCCTCACAA-3'. The sequence of miR-192-5p mimic was 5'-CUGACCU AUGAAUUGACAGCC-3', and the miR-192-5p inhibitor sequence was 5'-GGCUGUCAUAGUUAGGUCAG-3'. The FOXO1 siRNA was 5'-GGAGGUAUGAGUCA GUAUAUU-3'.

RNA isolation and quantitative RT-PCR

Total RNA was extracted with Trizol reagent (Thermo Fisher, Waltham, MA, USA) following the manufacturer's protocol, and reverse transcription polymerase chain reaction (RT-PCR) was performed using Premix Ex Taq DNA polymerase for real-time PCR (RR039B, Takara, Dalian, China). The RT primer for miR-192-5p was 5'-GTCGTATCCAGTGCAGGGTCCGAGGTATTC GCACTGGATACGACAGGCTGT-3'.

Quantitative PCR (qPCR) primers were as follows: circHIPK3 forward 5'-GGCAGCCTTACAGGGTTAAA-3', reverse 5'-GGGTAGACCAAGACTTGTGAGG-3', miR-192-5p forward, 5'-CTGACCTATGAATTG-3', reverse 5'-GTGCAGGGTCCGAGGT3'. U6 and GAPDH were used as internal control: U6 RT, 5'-GTC GTA TCC AGT GCA GGG TCC GAG GTA TTC GCA CTG GAT ACG ACA AAT ATG-3', U6 real-time PCR forward: 5'-CTCGCTTCGGCAGCACA-3', reverse, 5'-AACGCTTC ACGAATTTGCGT-3', GAPDH forward, 5'-GCTCTCT GCTCCTCCTGTTC-3', 5'-GACTCCGACCTTCACCT TCC-3'.

Pull down assay with biotinylated cicrHIPK3 DNA probe

Briefly, the biotin-labeled circHIPK3 DNA probe was designed (Thermo Fisher, Waltham, MA, USA), and dissolved in binding and washing buffer and mixed with M-280 streptavidin magnetic beads (Thermo Fisher) to generate probe-coated beads based on the manufacturer's guide. Cell lysates were mixed with the probe-coated beads. The RNAs combined to probe-coated beads were washed off and purified using qRT-PCR analysis. The wild-type and mutant circHIPK3 probe sequences were designed, and synthesized. In addition, random pull-down probe sequence used as negative control was 5'-Bio-TGCATCCAAGCCGATTGCGGTAACG-3'.

The biotin-labeled lncRNA DNA probe was designed (Thermo Fisher), dissolved in binding and washing buff-

er and mixed with M-280 streptavidin magnetic beads (Thermo Fisher) to generate probe-coated beads according to the manufacturer's instruction.

Immunohistochemistry

For histologic analysis, rats were sacrificed and tissues were fixed with 4% buffered paraformaldehyde for 24 h. Then they were embedded by using paraffin, and 5 μm thick continuous sections were obtained. H&E staining was carried out with the routine method in the lab.

Triglyceride, glucose and insulin analysis

Liver triglyceride (TG) was measured using commercial kits from Cayman chemical (Ann Arbor, Michigan, USA). Glucose tolerance tests were performed by intraperitoneal injection of D-glucose (Sigma-Aldrich) at a dose of 2.0 mg/g body weight after a 16 h fast. Pyruvate tolerance tests were performed by intraperitoneal injection of sodium pyruvate (Sigma-Aldrich) at a dose of 1.5 mg/g body weight after a 16 h fast. For insulin tolerance tests, mice were injected with regular human insulin (Sigma-Aldrich) at a dose of 1.0 U/kg body weight after a 6 h fast. Blood glucose levels were determined using a portable blood glucosemeter (Sigma-Aldrich). Plasma insulin levels were measured using commercial ELISA kits from R&D systems (Minneapolis, MN, USA).

Luciferase assay

Luciferase reporter experiments were performed as previously described [17]. Briefly, a 3'UTR segment of FOXO1/circHIPK3 and the mutant were amplified and validated prior to transfection in HepG2 cells or Huh7 cells. 100 nM miRNA mimic or mimic control (Thermo Fisher) were added to each well in 12-well plates. After 48 h treatment, cell lysates were prepared for luciferase activity measurement.

Western blotting

Western blotting was performed as described previously. Homogenized samples were boiled for 5 min in gel-loading buffer [125 mM Tris–HCl, pH 6.8, 4% sodium dodecyl sulfate (SDS), 10% 2-mercaptoethanol, 0.2% bromophenol blue] at a volume ratio of 1:1. Total-protein equivalents for each sample were separated *via* SDS-polyacrylamide gel electrophoresis (PAGE), as described by Laemmli, and transferred to PVDF membranes at 15 V for 1 h by using a semi-dry transfer system. Membranes were immediately placed into a blocking buffer (1% non-fat milk) in 10 mM Tris–HCl, pH 7.5, 100 mM NaCl, and 0.1% Tween-20. The blots were allowed to block at room temperature for 1 h and then incubated with specific primary antibodies at 25°C for 1 h, followed by an HRP-conjugated secondary antibody at 25°C for 1 h. Antibody labeling was detected using enhanced chemiluminescence according to the manufacturer's instructions.

Statistical analysis

The data in the study were shown as the mean ± standard deviation (SD). The data is analyzed by one-way analysis of variance (ANOVA) with Turkey's multiple comparison test or unpaired two-tailed Student's *t*-test, the differences will be considered significant when $p < 0.05$.

Results

CircHIPK3 promotes adipose deposition and TG accumulation in HepG2 cells

Firstly, we evaluated the effect of oleate on the expression of circHIPK3. As shown in Fig. 1A, oleate stimulated significant increase in circHIPK3 in HepG2 cells. We then synthesized circHIPK3 mimic and inhibitor, and evaluated their effects on circHIPK3 expression. Fig. 1B shows that circHIPK3 mimic significantly increased circHIPK3 level whereas anti-circHIPK3 significantly decreased circHIPK3 level in HepG2 cells. Fig. 1C shows that oleate significantly increased adipose deposition and TG content, and this stimulatory effect was significantly inhibited in the presence of anti-circHIPK3. In contrast, the co-treatment with circHIPK3 further enhanced the stimulatory effect of oleate on adipose content in HepG2 cells (Fig. 1C). Similarly, Fig. 1D shows that circHIPK3 increased TG content, whereas anti-circHIPK3 decreased TG content in HepG2 cells. Meanwhile, circHIPK3 and anti-circHIPK3 increased and decreased cellular glucose content, respectively, in FSK/DEX-treated HepG2 cells (Fig. 1E). Further mechanistic study shows that circHIPK3 increased mRNA level of PEPCK and G6Pase, two critical enzymes in gluconeogenesis, in FSK/DEX-treated HepG2 cells (Fig. 1F&G). In contrast, anti-circHIPK3 decreased mRNA level of PEPCK and G6Pase in FSK/DEX-treated HepG2 cells (Fig. 1F&G).

CircHIPK3 regulates miR-192-5p

We then evaluated the potential miRNA target of circHIPK3. As shown in Fig. 2A, bioinformatics assay shows that miR-192-5p shows strong binding potential with circHIPK3. We synthesized miR-192-5p and anti-miR-192-5p, and their efficiency was evaluated. Fig. 2B shows that miR-192-5p mimic significantly increased miR-192-5p, whereas anti-miR-192-5p significantly decreased miR-192-5p content in HepG2 cells and in Huh7 cells. Then the potential interaction between miR-192-5p and circHIPK3 was evaluated experimen-

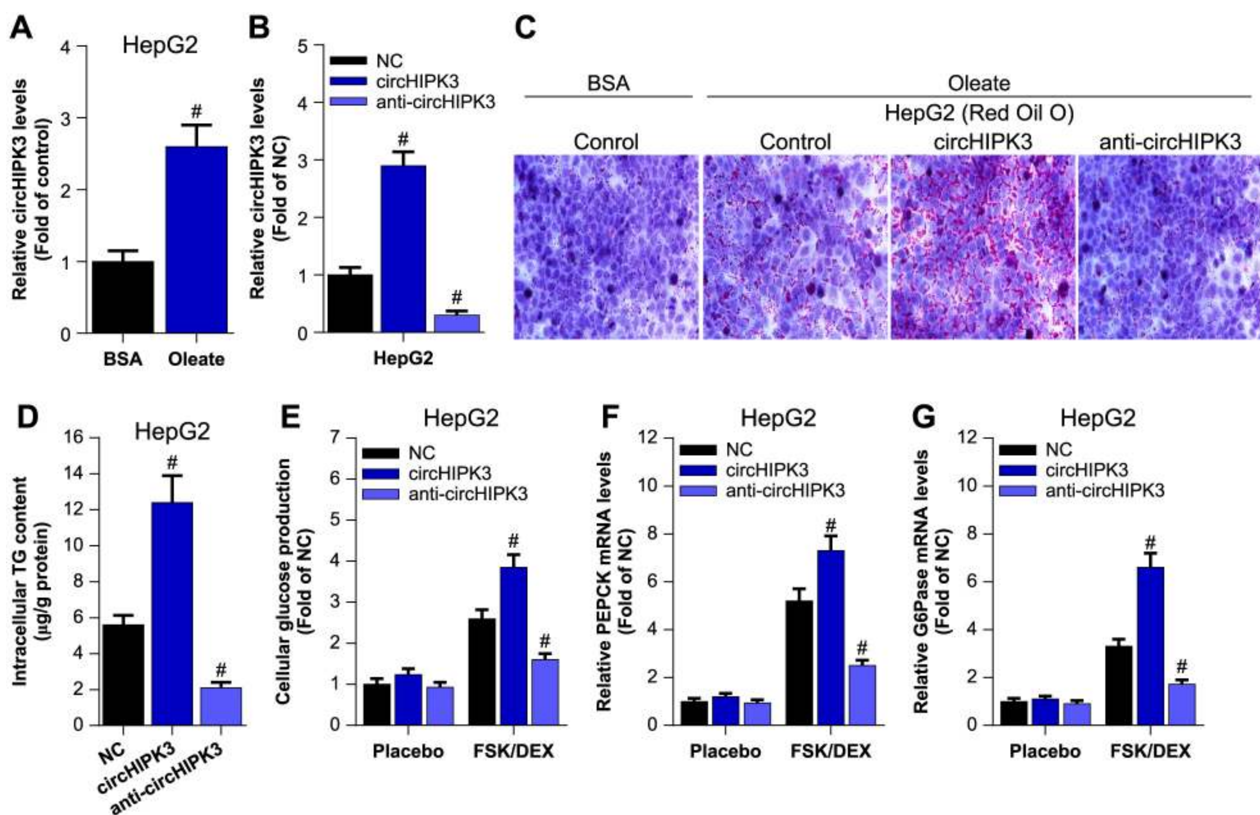

Fig. 1 CircHIPK3 is involved in lipid and glucose metabolism. (A) Summarized data showing that oleate (48 h) stimulated the expression of circHIPK3 in HepG2 cells in qPCR assay. (B) Summarized data showing the efficiency of circHIPK3 and anti-circHIPK3 (48 h) in HepG2 cells in qPCR assay. (C) Representative oil red O staining images showing the effect of circHIPK3 and anti-circHIPK3 on oleate-induced TG increase in HepG2 cells, oleate was added 48 h after transfection of each fragment, and the oleate treatment lasted for 48 h. (D) Summarized data showing the effect of circHIPK3 and anti-circHIPK3 on intracellular TG content in HepG2 cells in ELISA assay. (E) Summarized data showing the effect of circHIPK3 and anti-circHIPK3 on FSK/DEX-induced cellular glucose increase in HepG2 cells in ELISA assay. Summarized data showing the effect of circHIPK3 and anti-circHIPK3 on FSK/DEX-induced expression of PEPCK (F) and G6Pase (G) in HepG2 cells in qPCR assay. n = 5–6. $^{\#}p < 0.01$ *vs.* bovine serum albumin (BSA) group in A; $^{\#}p < 0.01$ *vs.* NC group in B–G.

tally. Fig. 2C shows that wild-type bio-circHIPK3 significantly increased enriched miR-192-5p, whereas the enrichment effect was totally lost when bio-circHIPK3 was mutant in HepG2 and AML12 cells. As shown in Fig. 2D&E, circHIPK3 luciferase reporter assay shows that miR-192-5p significantly decreased circHIPK3 luciferase activity, whereas anti-miR-192-5p significantly increased circHIPK3 luciferase activity in HepG2 cells and in Huh7 cells. Furthermore, miR-192-5p significantly decreased circHIPK3 level, whereas anti-miR-192-5p significantly increased circHIPK3 level in HepG2 cells and in Huh7 cells (Fig. 2F). Similarly, circHIPK3 significantly decreased miR-192-5p level, whereas anti-circHIPK3 significantly increased miR-192-5p level in HepG2 cells and in Huh7 cells (Fig. 2G & H). These results suggest that miR-192-5p and circHIPK3 work negatively.

MiR-192-5p regulates the expression of FOXO1 by targeting 3'UTR

Fig. 3A shows that oleate treatment significantly decreased miR-195-5p level in HepG2 cells. Consistently, miR-192-5p level was also decreased in the liver of diabetic db/db mice compared with that of control db/m mice (Fig. 3B). Bioinformatics assay shows that FOXO1 3'UTR is a potential binding site of miR-192-5p, we then constructed wild type and mutant FOXO1 3'UTR luciferase reporter vector (Fig. 3C). Fig. 3D shows that circHIPK3 overexpression significantly increased circHIPK3 level, whereas miR-192-5p significantly decreased circHIPK3 level in HepG2 and Huh7 cells. In contrast, circHIPK3 overexpression significantly decreased miR-192-5p level (Fig. 3D). FOXO1 luciferase assay shows that miR-192-5p significantly decreased luciferase activity, circHIPK3 significantly increased luciferase activity, and the co-treatment of cells with miR-192-5p and circHIPK3 did not change the luciferase

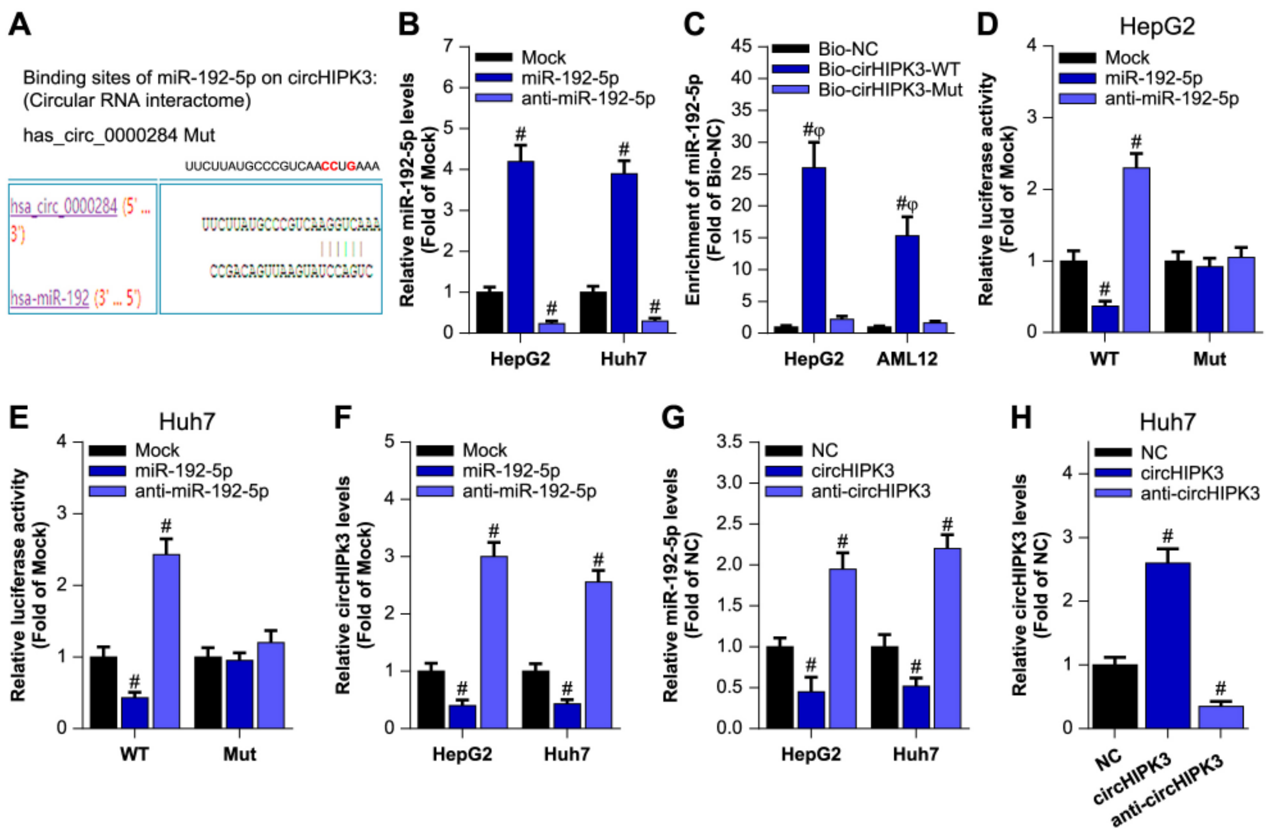

Fig. 2 miR-192-5p regulates circHIPK3. (A) The predicted binding site of miR-192-5p with circHIPK3 and the mutant site of circHIPK3. (B) qPCR was performed to evaluate the efficiency of miR-192-5p and anti-miR-192-5p in HepG2 cells and in Huh7 cells. (C) Enrichment of miR-192-5p by wild-type and mutant circHIPK3 in HepG2 cells and in AML12 cells. Effect of miR-192-5p and anti-miR-192-5p on luciferase activity in circHIPK3 luciferase reporter assay in HepG2 cells (D) and in Huh7 cells (E). (F) Effect of miR-192-5p and anti-miR-192-5p on circHIPK3 level in HepG2 cells and in Huh7 cells in qPCR assay. (G) Summarized data showing the effect of circHIPK3 and anti-circHIPK3 on miR-192-5p level in HepG2 cells and Huh7 cells in qPCR assay. (H) Summarized data showing the effect of circHIPK3 and anti-circHIPK3 on circHIPK3 level in Huh7 cells in qPCR assay. n = 5–6. $^{\#}p < 0.01$ *vs.* Mock group in B–F; $^{\#}p < 0.01$ *vs.* NC group in G; $^{\varphi}p < 0.01$ *vs.* Bio-circHIPK3 mutant group for HepG2 and Huh7 cells respectively in C.

activity; the inhibitory effect of miR-192-5p and the stimulatory effect of circHIPK3 on luciferase acitivty were lost when FOXO1 3'UTR was mutant (Fig. 3E). Similarly, miR-192-5p significantly decreased FOXO1 mRNA and protein level, whereas circHIPK3 significantly increased FOXO1 mRNA and protein level. In the presence of miR-192-5p and circHIPK3, however, FOXO1 mRNA and protein level remains unchanged (Fig. 3F&G). These results suggest that miR-192-5p regulates FOXO1 mRNA by targeting its 3'UTR, and that circHIPK3 regulates FOXO1 by buffering miR-192-5p.

Anti-miR-192-5p induces hepatic steatosis and insulin resistance through FOXO1

We then determined the relationship between miR-192-5p and FOXO1. As shown in Fig. 4A, anti-miR-192-5p significantly increased FOXO1 mRNA level. Fig. 4B shows that anti-miR-192-5p significantly increased blood glucose content. Similarly, anti-miR-192-5p significantly increased blood glucose during pyruvate and insulin injection (Fig. 4C&D). Similarly, anti-miR-192-5p significantly increased adipose deposition and TG content (Fig. 4E). Consistently, the anti-miR-192-5p significantly increased the mRNA level of PEPCK, G6Pase, SREBP-1c and FAS (Fig. 4F&G). Notably, the effect of anti-miR-192-5p on blood glucose content, blood glucose metabolism, and the expression of PEPCK/G6Pase/SREBP-1c/FAS was significantly inhibited by FOXO1 shRNA. These results suggest that anti-miR-192-5p induced hepatic steatosis and insulin resistance through FOXO1.

CircHIPK3 reverses the inhibitory effect of miR-192-5p and coordinates the regulation of glycolipid metabolism in hepatocytes

Finally, we evaluated the relationship between miR-192-5p and circHIPK3. As shown in Fig. 5A&B, miR-192-5p significantly decreased adipose deposition and

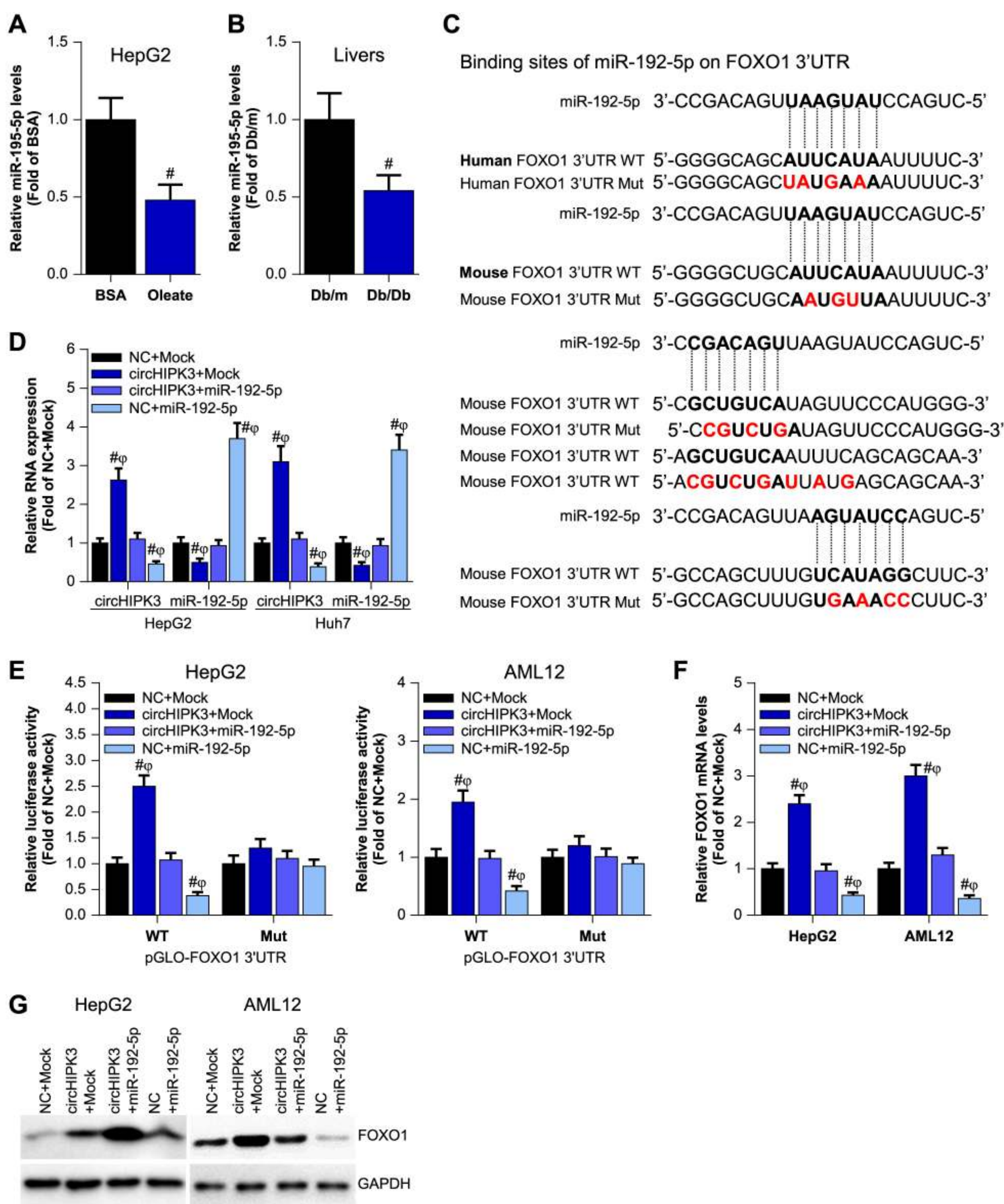

Fig. 3 miR-192-5p regulates the expression of FOXO1 by targeting 3'UTR. (A) Summarized data showing the effect of oleate on miR-195-5p in HepG2 cells in qPCR assay. (B) miR-192-5p level was decreased in the liver of diabetic db/db mice compared with that from control db/m mice. (C) The binding sites of miR-192-5p with FOXO1 3'UTR and the construction of mutants of FOXO1 3'UTR. (D) Summarized data showing the effect of circHIPK3 overexpression and miR-192-5p on the circHIPK3 and miR-192-5p level in in HepG2 cells and in AML12 cells. (E) Luciferase reporter gene system was used to detect the effect of cicrHIPK3 and miR-192-5p on FOXO1 3'UTR luciferase activity in HepG2 cells and in AML12 cells. (F) Summarized data showing the effect of circHIPK3 and miR-192-5p on FOXO1 mRNA level in HepG2 cells and in AML12 cells in qPCR assay. (G) Representative western blot images showing the effect of circHIPK3 and miR-192-5p on FOXO1 protein level in HepG2 cells and in AML12 cells. n = 5–6. $^{\#}p < 0.01$ *vs.* BSA group in A; $^{\#}p < 0.01$ *vs.* Db/m group in B; $^{\#}p < 0.01$ *vs.* NC + Mock group in D-F; $^{\varphi}p < 0.01$ *vs.* miR-192-5p + circHIPK3 group in D–F.

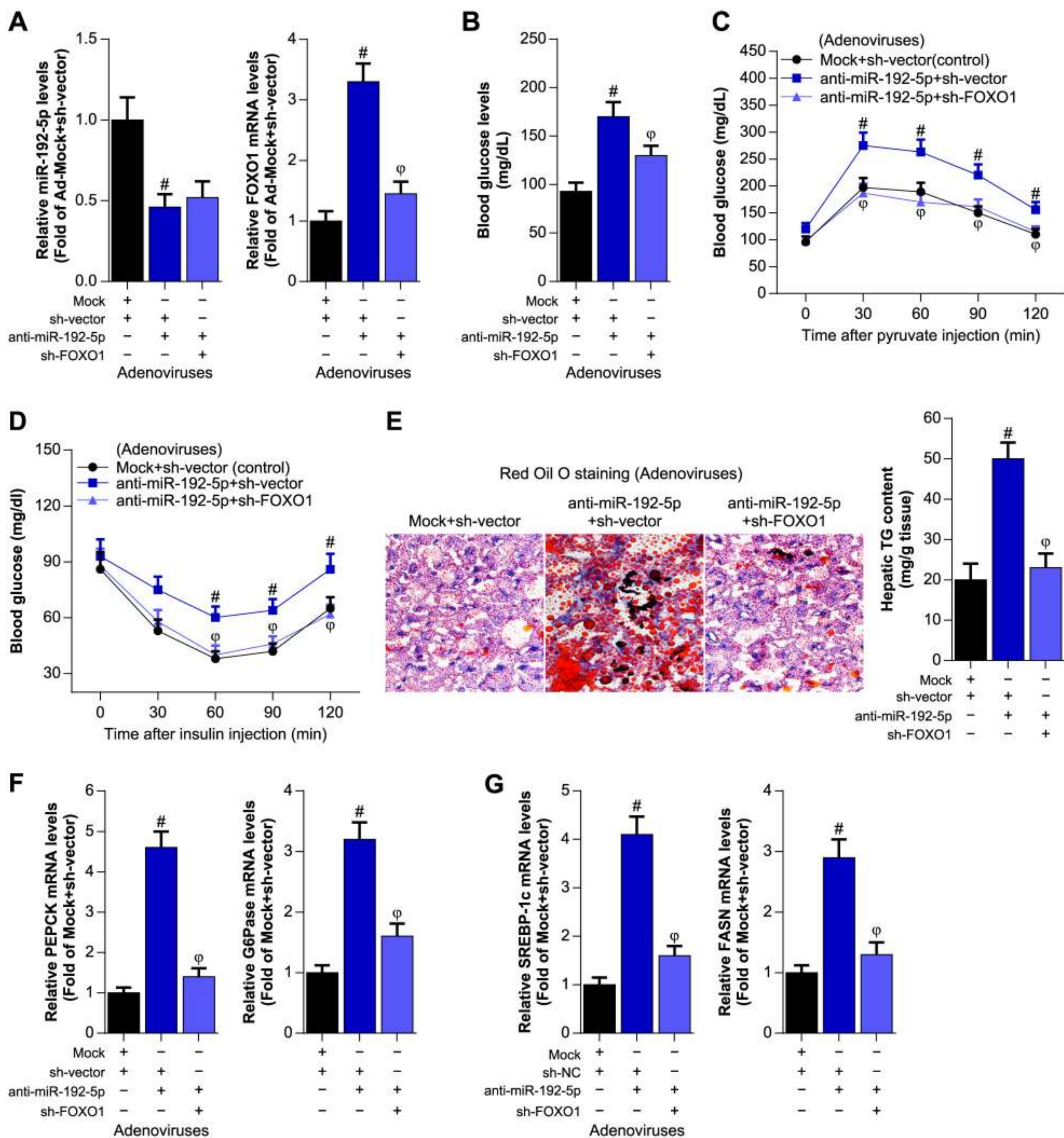

Fig. 4 FOXO1 shRNA inhibits miR-192-5p-induced hepatic steatosis and insulin resistance. (A) Summarized data showing the effect of anti-miR-192-5p and FOXO1 shRNA on miR-192-5p level (left panel) and FOXO1 mRNA level (right panel) in qPCR assay. (B) Summarized data showing the effect of anti-miR-192-5p and FOXO1 shRNA on blood glucose level in ELISA assay. Summarized data showing that FOXO1 shRNA reversed anti-miR-192-5p-inducd blood glucose increase after pyruvate (C) and insulin injection (D). (E) Inhibitory effect of FOXO1 shRNA on anti-miR-192-5p-inducd adipose deposition in mouse liver. (F) Summarized data showing the inhibitory effect of FOXO1 shRNA on anti-miR-192-5p-inducd expression of PEPCK and G6Pase in mouse liver in qPCR assay. (G) Summarized data showing the inhibitory effect of FOXO1 shRNA on anti-miR-192-5p-inducd expression of SREBP-1c and FAS in mouse liver in qPCR assay. $n = 5–6$. $^{\#}p < 0.01$ *vs.* sh-vector + Mock group, $^{\varphi}p < 0.01$ *vs.* sh-vector + anti-miR-192-5p group in A–G.

TG content in HepG2 cells, which was significantly reversed by the co-treatment with circHIPK3. As shown in Fig. 5C, FSK/DEX significantly increased cellular glucose, mRNA level of PEPCK and G6Pase, and this stimulatory effect of FSK/DEX was significantly inhibited by miR-192-5p. In the presence of circHIPK3, however, the inhibitory effect of miR-192-5p was totally lost (Fig. 5C&D&E). These results suggest that miR-192-5p

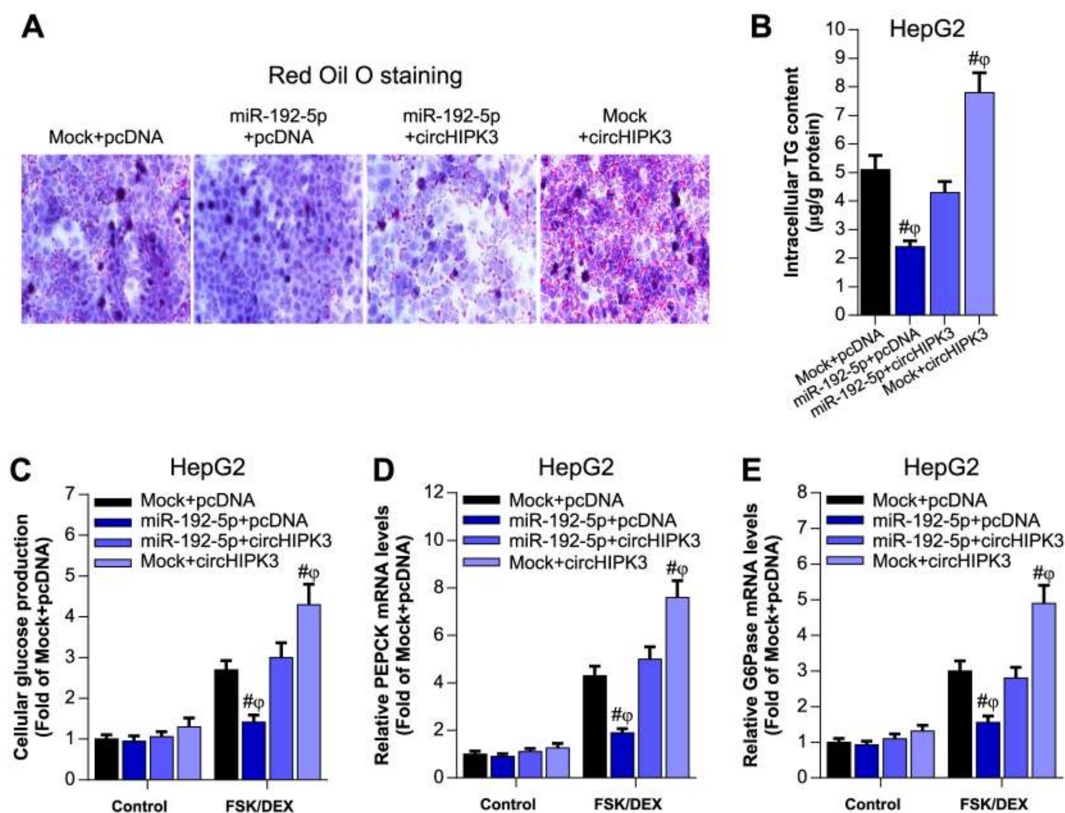

Fig. 5 miR-192-5p and circHIPK3 coordinate the regulation of glycolipid metabolism in HepG2 cells. (A) Representative red oil O staining showing that the inhibitory effect of miR-192-5p on accumulation of lipid droplets was reversed by circHIPK3 in HepG2 cells. Summarized data showing that the inhibitory effect of miR-192-5p on TG content (B) and cellular glucose production (C) was reversed by circHIPK3 in HepG2 cells. Summarized data showing the effect of circHIPK3 or anti-circHIPK3 on FSK/DEX-induced expression of PEPCK (D) and G6Pase (E) in HepG2 cells in qPCR assay. $n = 5–6$. $^{\#}p < 0.01$ *vs.* Mock + pcDNA group, $^{\varphi}p < 0.01$ *vs.* miR-192-5p + circHIPK3 group in B–E.

and circHIPK3 coordinates the regulation of glycolipid metabolism in hepatocytes.

Discussion

In the present study, we evaluated the involvement of circHIPK3 in hyperglycemia and insulin resistance. It was found that oleate significantly increased circHIPK3, which enhanced the stimulatory effect of oleate on adipose deposition, TG content, and cellular glucose content in HepG2 cells. Further study demonstrated that circHIPK3 exerts its regulatory effect by sponging miR-192-5p. In contrast, miR-192-5p could target and degrade FOXO1 mRNA, thereby decreasing its expression. Importantly, this circHIPK3-miR-192-5p-FOXO1 signaling pathway was involved in hyperglycemia and insulin resistance.

It has been documented that circHIPK3 was involved in proliferation, migration, and development of cancer. For example, it has been reported that circHIPK3 was increased in colorectal cancer, and functionally knockdown of circHIPK3 markedly inhibited colorectal cancer cells proliferation, migration, invasion, and induced apoptosis *in vitro* and suppressed colorectal cancer growth and metastasis *in vivo* [18]. Further study shows that circHIPK3 exerted its function by sponging miR-7 [18]. Zheng *et al.* demonstrated that circHIPK3 was involved in human cell growth, and that circHIPK3 was observed to sponge to 9 miRNAs with 18 potential binding sites [5]. Another study demonstrated that inhibition of circHIPK3 prevents angiotensin II-induced cardiac fibrosis by sponging miR-29b-3p [19]. In consistent with these studies, the present study demonstrated that circHIPK3 was increased in response to oleate stimulation, and that circHIPK3 exerted its effect by sponging miR-192-5p. These studies suggest that circHIPK3 may have multiple functions in different cell types.

It has been shown that miR-192-5p could bind with various targets in different types of tissues and cells. For example, it has been reported that H_2O_2 treatment promoted the production of miR-192-5p, and that miR-192-5p-targeted genes were involved in cell cycle, DNA repair and stress response. Accordingly, miR-192-5p overexpression significantly decreased pro-

liferation, inducing cell death of endothelial cells [20]. A recent study shows that miR-192-5p targets the mRNA for ATP1B1 (β1 subunit of Na^+/K^+-ATPase), thereby leading to decreased Na^+/K^+-ATPase-mediated renal tubular reabsorption and decreased blood pressure [21]. In consistent with these studies, the present study shows that miR-192-5p could target FOXO1, and its dysregulation was involved in hyperglycemia and insulin resistance. Indeed, it has been shown that the expression of FOXO1 and acetylated-FOXO1 is regulated by miR-96-5p in human breast cancer cell [13]. These studies suggest that the expression of FOXO1 is regulated by different miRNAs.

In summary, the present study demonstrated that increased circHIPK3 could target miR-192-5p, which then targets and degrades FOXO1 mRNA, thereby decreasing its expression. Considering the importance of FOXO1 in hyperglycemia and insulin resistance, this circHIPK3-miR-192-5p-FOXO1 signaling pathway may provide new insight on the initiation and development of these diseases.

Disclosure

None.

Supplemental data

1. circHIPK3 sequence (Homo sapiens):

>hg19_hub_1_memczak_circRNAs range = chr11: 33307959-33309057 5'pad=0 3'pad=0 strand=+ repeat Masking=none

GTATGGCCTCACAAGTCTTGGTCTACCCACCATAT
GTTTATCAAACTCAGTCAAGTGCCTTTTGTAGTG
TGAAGAAACTCAAAGTAGAGCCAAGCAGTTGTG
TATTCCAGGAAAGAAACTATCCACGGACCTATGT
GAATGGTAGAAACTTTGGAAATTCTCATCCTCCC
ACTAAGGGTAGTGCTTTTCAGACAAAGATACCAT
TTAATAGACCTCGAGGACACAACTTTTCATTGCA
GACAAGTGCTGTTGTTTTGAAAAACACTGCAGG
TGCTACAAAGGTCATAGCAGCTCAGGCACAGCA
AGCTCACGTGCAGGCACCTCAGATTGGGGCGTG
GCGAAACAGATTGCATTTCCTAGAAGGCCCCCA
GCGATGTGGATTGAAGCGCAAGAGTGAGGAGTT
GGATAATCATAGCAGCGCAATGCAGATTGTCGAT
GAATTGTCCATACTTCCTGCAATGTTGCAAACCA
ACATGGGAAATCCAGTGACAGTTGTGACAGCTA
CCACAGGATCAAAACAGAATTGTACCACTGGAG
AAGGTGACTATCAGTTAGTACAGCATGAAGTCTT
ATGCTCCATGAAAAATACTTACGAAGTCCTTGAT
TTTCTTGGTCGAGGCACGTTTGGCCAGGTAGTTA
AATGCTGGAAAAGAGGGACAAATGAAATTGTAG
CAATCAAAATTTTGAAGAATCATCCTTCTTATGCC
CGTCAAGGTCAAATAGAAGTGAGCATATTAGCAA
GGCTCAGTACTGAAAATGCTGATGAATATAACTT
TGTACGAGCTTATGAATGCTTTCAGCACCGTAAC
CATACTTGTTTAGTCTTTGAGATGCTGGAACAAA
ACTTGTATGACTTTCTGAAACAAAATAAATTTAG
TCCCCTGCCACTAAAAGTGATTCGGCCCATTCTT
CAACAAGTGGCCACTGCACTGAAAAAATTGAAA
AGTCTTGGTTTAATTCATGCTGATCTCAAGCCAG
AGAATATTATGTTGGTGGATCCTGTTCGGCAGCC
TTACAGGGTTAAAGTAATAGACTTTGGGTCGGCC
AGTCATGTATCAAAGACTGTTTGTTCAACATATCT
ACAATCTCGGTACTACAG

2. FOXO1 3'UTR sequence (Homo sapiens):

GGGTTAGTGAGCAGGTTACACTTAAAAGTACTTC
AGATTGTCTGACAGCAGGAACTGAGAGAAGCAG
TCCAAAGATGTCTTTCACCAACTCCCTTTTAGTTT
TCTTGGTTAAAAAAAAAAAACAAAAAAAAAAAACC
CTCCTTTTTTCCTTTCGTCAGACTTGGCAGCAAA
GACATTTTTCCTGTACAGGATGTTTGCCCAATGT
GTGCAGGTTATGTGCTGCTGTAGATAAGGACTGT
GCCATTGGAAATTTCATTACAATGAAGTGCCAAA
CTCACTACACCATATAATTGCAGAAAAGATTTTC
AGATCCTGGTGTGCTTTCAAGTTTTGTATATAAGC
AGTAGATACAGATTGTATTTGTGTGTGTTTTTGGT
TTTTCTAAATATCCAATTGGTCCAAGGAAAGTTTA
TACTCTTTTTGTAATACTGTGATGGGCCTCATGTC
TTGATAAGTTAAACTTTTGTTTGTACTACCTGTTT
TCTGCGGAACTGACGGATCACAAAGAACTGAAT
CTCCATTCTGCATCTCCATTGAACAGCCTTGGAC
CTGTTCACGTTGCCACAGAATTCACATGAGAACC
AAGTAGCCTGTTATCAATCTGCTAAATTAATGGAC
TTGTTAAACTTTTGGAAAAAAAAAAGATTAAATGC
CAGCTTTGTACAGGTCTTTTCTATTTTTTTTTGTT
TATTTTGTTATTTGCAAATTTGTACAAACATTTAA
ATGGTTCTAATTTCCAGATAAATGATTTTTGATGT
TATTGTTGGGACTTAAGAACATTTTTGGAATAGAT
ATTGAACTGTAATAATGTTTTCTTAAAACTAGAGT
CTACTTTGTTACATAGTCAGCTTGTAAATTTTGTG
GAACCACAGGTATTTGGGGCAGCATTCATAATTT
TCATTTTGTATTCTAACTGGATTAGTACTAATTTTA
TACATGCTTAACTGGTTTGTACACTTTGGGATGCT
ACTTAGTGATGTTTCTGACTAATCTTAAATCATTG
TAATTAGTACTTGCATATTCAACGTTTCAGGCCCT
GGTTGGGCAGGAAAGTGATGTATAGTTATGGACA
CTTTGCGTTTCTTATTTAGGATAACTTAATATGTTT
TTATGTATGTATTTTAAAGAAATTTCATCTGCTTCT
ACTGAACTATGCGTACTGCATAGCATCAAGTCTT
CTCTAGAGACCTCTGTAGTCCTGGGAGGCCTCAT
AATGTTTGTAGATCAGAAAAGGGAGATCTGCATC
TAAAGCAATGGTCCTTTGTCAAACGAGGGATTTT
GATCCACTTCACCATTTTGAGTTGAGCTTTAGCA
AAAGTTTCCCCTCATAATTCTTTGCTCTTGTTTCA

GTCCAGGTGGAGGTTGGTTTTGTAGTTCTGCCTT
GAGGAATTATGTCAACACTCATACTTCATCTCATT
CTCCCTTCTGCCCTGCAGATTAGATTACTTAGCAC
ACTGTGGAAGTTTAAGTGGAAGGAGGGAATTTA
AAAATGGGACTTGAGTGGTTTGTAGAATTTGTGT
TCATAAGTTCAGATGGGTAGCAAATGGAATAGAA
CTTACTTAAAAATTGGGGAGATTTATTTGAAAAC
CAGCTGTAAGTTGTGCATTGAGATTATGTTAAAA
GCCTTGGCTTAAGAATTTGAAAATTTCTTTAGCC
TGTAGCAACCTAAACTGTAATTCCTATCATTATGT
TTTATTACTTTCCAATTACCTGTAACTGACAGACC
AAATTAATTGGCTTTGTGTCCTATTTAGTCCATCA
GTATTTTCAAGTCATGTGGAAAGCCCAAAGTCAT
CACAATGAAGAGAACAGGTGCACAGCACTGTTC
CTCTTGTGTTCTTGAGAAGGATCTAATTTTTCTGT
ATATAGCCCACATCACACTTGCTTTGTCTTGTATG
TTAATTGCATCTTCATTGGCTTGGTATTTCCTAAAT
GTTTAACAAGAACACAAGTGTTCCTGATAAGATT
TCCTACAGTAAGCCAGCTCTATTGTAAGCTTCCC
ACTGTGATGATCATTTTTTTGAAGATTCATTGAAC
AGCCACCACTCTATCATCCTCATTTTGGGGCAGT
CCAAGACATAGCTGGTTTTAGAAACCCAAGTTCC
TCTAAGCACAGCCTCCCGGGTATGTAACTGAACT
TGGTGCCAAAGTACTTGTGTACTAATTTCTATTAC
TACGTACTGTCACTTTCCTCCCGTGCCATTACTGC
ATCATAATACAAGGAACCTCAGAGCCCCCATTTG
TTCATTAAAGAGGCAACTACAGCCAAAATCACTG
TTAAAATCTTACTACTTCATGGAGTAGCTCTTAGG
AAAATATATCTTCCTCCTGAGTCTGGGTAATTATA
CCTCTCCCAAGCCCCCATTGTGTGTTGAAATCCT
GTCATGAATCCTTGGTAGCTCTCTGAGAACAGTG
AAGTCCAGGGAAAGGCATCTGGTCTGTCTGGAA
AGCAAACATTATGTGGCCTCTGGTAGTTTTTTTCC
TGTAAGAATACTGACTTTCTGGAGTAATGAGTAT
ATATCAGTTATTGTACATGATTGCTTTGTGAAATG
TGCAAATGATATCACCTATGCAGCCTTGTTTGATT
TATTTTCTCTGGTTTGTACTGTTATTAAAAGCATAT
TGTATTATAGAGCTATTCAGATATTTTAAATATAAA
GATGTATTGTTTCCGTAATATAGACGTATGGAATA
TATTTAGGTAATAGATGTATTACTTGGAAAGTTCT
GCTTTGACAAACTGACAAAGTCTAAATGAGCAC
ATGTATCCCAGTGAGCAGTAAATCAATGGAACAT
CCCAAGAAGAGGATAAGGATGCTTAAAATGGAA
ATCATTCTCCAACGATATACAAATTGGACTTGTTC
AACTGCTGGATATATGCTACCAATAACCCCAGCC
CCAACTTAAAATTCTTACATTCAAGCTCCTAAGA
GTTCTTAATTTATAACTAATTTTAAAAGAGAAGTT
TCTTTTCTGGTTTTAGTTTGGGAATAATCATTCAT
TAAAAAAAATGTATTGTGGTTTATGCGAACAGAC
CAACCTGGCATTACAGTTGGCCTCTCCTTGAGGT
GGGCACAGCCTGGCAGTGTGGCCAGGGGTGGCC
ATGTAAGTCCCATCAGGACGTAGTCATGCCTCCT
GCATTTCGCTACCCGAGTTTAGTAACAGTGCAGA
TTCCACGTTCTTGTTCCGATACTCTGAGAAGTGC
CTGATGTTGATGTACTTACAGACACAAGAACAAT
CTTTGCTATAATTGTATAAAGCCATAAATGTACAT
AAATTATGTTTAAATGGCTTGGTGTCTTTCTTTTC
TAATTATGCAGAATAAGCTCTTTATTAGGAATTTT
TTGTGAAGCTATTAAATACTTGAGTTAAGTCTTGT
CAGCCA

Mus musculus FOXO1 3'UTR:
GAGTTAGTGAGCAGGCTACATTTAAAAGTCCTTC
AGATTGTCTGACAGCAGGAACTGAGGAGCAGTC
CAAAGATGCCCTTCACCCCTCCTTATAGTTTTCA
AGATTTAAAAAAAAAAAAAAAAAAAAAAAAG
TCCTTTCTCCTTTCCTCAGACTTGGCAACAGCGG
CAGCACTTTCCTGTGCAGGATGTTTGCCCAGCGT
CCGCAGGTTTTGTGCTCCTGTAGATAAGGACTGT
GCCATTGGGAATCATTACAATGAAGTGCCAAACT
CACTACACCATGTAATTGCAGAAAAGACTTTCAG
ATCCTGGAGTGCTTTCAAGTTTTGTATATATGCAG
TAGATACAGAATTGTATTTGTGTGTGTGTTTTTTA
ATACCTACTTGGTCCAAGGAAAGTTTATACTCTTT
TGTAATACTGTGATGGTCTCAAGTCTTGATAAACT
TTGCTTTGTACTACCTGTGTTCTGCTACAGTGAG
AAGTCATGAACTAAGATCTCTGTCCTGCACCTCG
GCTGAATGACTGAACCTGGTCATTTGCCACAGAA
CCCATGAGAGCCAAGTAGCCAGTGATCAATGTGC
TGAATTAATGGACTTGTCAAACTTTGGGGCAGAA
TAAGATTAAGTGCCAGCTTTGTACAGGTCTTTTT
CTATTGTTTTTGTTGTTGTTTATTTTGTTATTTGCA
AATTTGTACAAACAACTTAAAATGGTTCTAATTTC
CAGATAAATGACTTTTGATGTTATTGTTAGGACTC
AACATCTTTTGGAATAGATACCGAAGTGTAATGT
TTTCTTAAAACTAGAGTCTACTTTGTTACATTGTC
TGCTTATAAATTTGTGAAATCAGAGGTATTTGGG
GGCTGCATTCATAATTTTCATTTTGTATTTCTAACT
GGATTAGTACTAATTTTATATGTGCTCAGCTGGTT
TGTACACTTTGCGATGATACCTGATAATGTTTCTG
ACTAATCGTAAACCATTGTAATTAGTACTTGCACA
CTCAACGTTCCTGGCCCTTTGGGCAGGAAAGTTA
TGTATAGTTACAGACACTCTGTTTTGTGTGTAGAT
TTATGTGTGTATTTTAAAGAAATTTCACCTGCTTT
TATTACCCTGTGAGTTGTGTACAGCGCATAGCAC
CAAGTCTTCAGATAGATGCCACGTGCTTACAGCC
TTCTAGGGAAGCCTGCCAGATGATGCCCTGTGTC
ACGCTGTCATAGTTCCCATGGGAACTCTGTCTGT
CGCTCAGGAAAGGGGAACTTTTATCTAAGGTGAT
GTTCTTTGTCTGACTGGGGTTCGCCTCCTACTAC
TCTGAGCTGTTGGCTTTTGTCACGATGGAGGTGG
CTTTGTGGCTCTGTCCTGAAGAATCCTGTCACTT
CTCGGTCCCCACCTCTGTTCTCTTTGGCTCTGAA
CAGTGTAAATCTAAGGAGGAAGTTTACAAATAGG
ACTTCAGTGATTTATGGAGTGCTCTGTGCGCCTA
AGTACAGACAGTGGCAGGATTAGTTAAAAATGA

AGGCAGTAAACTTGGAAACCAGCCAGCTATAAA
TGGACATTTATTTTGAAATCCTTAGCTTAAGAATT
TGAGAAGTTTTTTCAGCCTTGAGCAGCCTAATGT
GTCTCAAACATTTACGTTTTTTATACATTCTATTTA
CCTGAAATCCTGCCAGACCAGGATAATTGGTTTT
ACCTCTCATTCCGTCCATCGGTGTTTCCCAGTCTC
CCACAGTTTGAGGAATAGATGTACCCCAGCACCC
CTCTTTGCCTTTATGAGAAGGCCTGGTTTGCATG
AGAAGACCAAATTGCACTTCCATGAGAAGACCA
AATTGTTTGTAGTGTTACTTAGCTCTCCCCTCGTT
TGTTAGTGTGTGTTAACAAGAATAAAATGTCCCT
GCTTTCACCCACCGTTGGCCAGCTTTGTCATAGG
CTTCCCACCATAACTTTCACTATTTTAAACACATA
TTGAGCCACTGCTCGTCTGACTACCTTTGTTTGG
GCACTCCAAAACAGGACTTGTTTTAGAAATGAA
CTCCTCCAAGTAGAGCCTCCTTCAAACAGAGTA
GAATTTCCTGGTGTCAAAGAACCCGGGTCTGTCT
CCCTTTCCTCCTCCCTCTGCCATTTCTTACCATTG
CGGAAAGAGAGAGCCTCCGTGTGTAATCATTCA
GTAGAGGCAGCTACCGCCCTGGCAGTGGTCTAC
CTGCTGAATGCCACTGAATGACTAGGAGGTGTCT
CTCCCTTCAGAAGCTGTCAATTTCAGCAGCAACC
CCTGTTTTCCTTGGTGTTAAGATCCCAGTGTGAA
TCATGGGCAGTTGTCTGGGGCACAGTGAACTCC
AGGAAAGGCTTCGTATCTGTTTTGAAAACAAAC
ATCAAACGTGTGAGCTCCGAGGGTCCTTTTCTGG
GAGAATGTTCGCTTTCTGGTCTATTATTGTACATG
ATTGCTCTGTGAAAAGACTTCATCTATGCAGCCT
TGTTTGATTCATTTCCTTTGGTGTGTTCTGTTGTT
AAGAGCAAATTGTATTATAGAGCTATTTGGATATT
TTAAATATAAAGATGTATTGTTTCCATAATATAGAT
GTATGGAGTATATTTAGGTGATAGATGTACAACTT
GGAAAGTTCTGCTTGGACAAACTGAGTCTAAGT
TAATTAGCAAATAATATATCCTGATGAGCAGGAAG
CCCTGAAACCTAACAACAGTAAGCGGAGAAAAT
CACTTAAAATGGAAACAGTTCCCCAAAGGTGTT
CAATTTGAACTTGTTCAACTGCTTAATATATGGTC
CCCCCCCCCCCCAAAAAAAAAACCTTGAAGTTC
TTAGTTTTCAGCTCTCCAAGTTACTGATTTTAAGT
GAAGTTTCTCTGTGGTTTCAGCTGGGGAGTGATT
GTTCAGTAGAGTGTGCATTGTGCTTTATGCAAAC
CAAACAGCCTGGCCCTGTGGCCGGGGACAGACA
GACAGCCCGTCAGGATAGAGTCCCGCCCTTCGC
CACCACAGCGGACTTGAGTAACAGTGCAGATGC
CTTGCTCCTGTTCCATTGCTATCTGAGAAGTGCCT
GATGAGGATGGTAAACTTACAGACACAAGAACA
ATCCTTACTGTGCGTTGTATAAAGCCATAAATGTA
CATAAATCATCTTAAGTGGC//

References

1. Wu Z, Huang W, Wang X, Wang T, Chen Y, *et al.* (2018) Circular RNA CEP128 acts as a sponge of miR-145-5p in promoting the bladder cancer progression *via* regulating SOX11. *Mol Med* 24: 40.
2. Huang M, Zhong Z, Lv M, Shu J, Tian Q, *et al.* (2016) Comprehensive analysis of differentially expressed profiles of lncRNAs and circRNAs with associated co-expression and ceRNA networks in bladder carcinoma. *Oncotarget* 7: 47186–47200.
3. Shang X, Li G, Liu H, Li T, Liu J, *et al.* (2016) Comprehensive circular RNA profiling reveals that hsa_circ_0005075, a new circular RNA biomarker, is involved in hepatocellular crcinoma development. *Medicine (Baltimore)* 95: e3811.
4. Zhong Z, Huang M, Lv M, He Y, Duan C, *et al.* (2017) Circular RNA MYLK as a competing endogenous RNA promotes bladder cancer progression through modulating VEGFA/VEGFR2 signaling pathway. *Cancer Lett* 403: 305–317.
5. Zheng Q, Bao C, Guo W, Li S, Chen J, *et al.* (2016) Circular RNA profiling reveals an abundant circHIPK3 that regulates cell growth by sponging multiple miRNAs. *Nat Commun* 7: 11215.
6. Cheng Z, White MF (2011) Targeting forkhead box O1 from the concept to metabolic diseases: lessons from mouse models. *Antioxid Redox Signal* 14: 649–661.
7. Chen S, Villalta SA, Agrawal DK (2016) FOXO1 mediates vitamin D deficiency-induced insulin resistance in skeletal muscle. *J Bone Miner Res* 31: 585–595.
8. Matsumoto M, Han S, Kitamura T, Accili D (2006) Dual role of transcription factor FoxO1 in controlling hepatic insulin sensitivity and lipid metabolism. *J Clin Invest* 116: 2464–2472.
9. Song Y, Wu L, Li M, Xiong X, Fang Z, *et al.* (2019) Down-regulation of MicroRNA-592 in obesity contributes to hyperglycemia and insulin resistance. *EBioMedicine* 42: 494–503.
10. Wang Y, Viscarra J, Kim SJ, Sul HS (2015) Transcriptional regulation of hepatic lipogenesis. *Nat Rev Mol Cell Biol* 16: 678–689.
11. Honma M, Sawada S, Ueno Y, Murakami K, Yamada T, *et al.* (2018) Selective insulin resistance with differential expressions of IRS-1 and IRS-2 in human NAFLD livers. *Int J Obes (Lond)* 42: 1544–1555.
12. Higuchi N, Kato M, Shundo Y, Tajiri H, Tanaka M, *et al.* (2008) Liver X receptor in cooperation with SREBP-1c is a major lipid synthesis regulator in nonalcoholic fatty liver disease. *Hepatol Res* 38: 1122–1129.
13. Shi Y, Zhao Y, Shao N, Ye R, Lin Y, *et al.* (2017) Overexpression of microRNA-96-5p inhibits autophagy and apoptosis and enhances the proliferation, migration and invasiveness of human breast cancer cells. *Oncol Lett* 13: 4402–4412.
14. Jaeger A, Zollinger L, Saely CH, Muendlein A,

Evangelakos I, *et al.* (2018) Circulating microRNAs -192 and -194 are associated with the presence and incidence of diabetes mellitus. *Sci Rep* 8: 14274.

15. Meex SJ, Andreo U, Sparks JD, Fisher EA (2011) Huh-7 or HepG2 cells: which is the better model for studying human apolipoprotein-B100 assembly and secretion? *J Lipid Res* 52: 152–158.
16. Tikhanovich I, Cox J, Weinman SA (2013) Forkhead box class O transcription factors in liver function and disease. *J Gastroenterol Hepatol* 28 Suppl 1: 125–131.
17. Aldred SF, Collins P, Trinklein N (2011) Identifying targets of human micrornas with the LightSwitch Luciferase Assay System using 3'UTR-reporter constructs and a microRNA mimic in adherent cells. *J Vis Exp* 55: 3343.
18. Zeng K, Chen X, Xu M, Liu X, Hu X, *et al.* (2018) CircHIPK3 promotes colorectal cancer growth and metastasis by sponging miR-7. *Cell Death Dis* 9: 417.
19. Ni H, Li W, Zhuge Y, Xu S, Wang Y, *et al.* (2019) Inhibition of circHIPK3 prevents angiotensin II-induced cardiac fibrosis by sponging miR-29b-3p. *Int J Cardiol* 292: 188–196.
20. Fuschi P, Carrara M, Voellenkle C, Garcia-Manteiga JM, Righini P, *et al.* (2017) Central role of the p53 pathway in the noncoding-RNA response to oxidative stress. *Aging (Albany NY)* 9: 2559–2586.
21. Baker MA, Wang F, Liu Y, Kriegel AJ, Geurts AM, *et al.* (2019) MiR-192-5p in the kidney protects against the development of hypertension. *Hypertension* 73: 399–406.